
HOW POISONING IS AVOIDED IN A STEP OF RELEVANCE TO THE HABER-BOSCH CATALYSIS

Shivam Tripathi^{1,2}, Luigi Bonati¹, Simone Perego^{1,3}, and Michele Parrinello^{1*}

¹ Atomistic Simulations, Italian Institute of Technology, Genova, Italy

² Department of Materials Science and Engineering, Indian Institute of Technology Kanpur, Uttar Pradesh, India

³ Department of Materials Science, University of Milano-Bicocca, Milano, Italy

*Corresponding Author: Michele Parrinello (michele.parrinello@iit.it)

ABSTRACT

For a catalyst to be efficient and durable, it is crucial that the reaction products do not poison the catalyst. In the case of the Haber-Bosch iron based catalyst, the rate-limiting step is believed to be the decomposition of nitrogen molecules on the Fe(111) surface. This step leads to the production of atomic nitrogen on the surface N^* that unless are hydrogenated and eventually released as NH_3 molecules, remain on the surface. Thus, it is important to ascertain how a high N^* coverage affects nitrogen dissociative chemisorption. To answer this question, we study the properties of the Fe(111) surface at different N^* coverage both at room and *operando* temperature. Using state-of-the-art simulations, we have already found that, at high temperatures, the surface atoms are highly mobile and that the catalytic centers normally associated with the surface activity acquire a finite lifetime [1]. Here, we discover that the N^* surface atoms are highly mobile and that coverage reduces but does not eliminate iron mobility. The N^* atoms promote the formation of metastable iron triangular surface structures whose chemical composition can be described as $Fe_3^*N_i^*$ $i = 1, 4$. These structures are the result of the frustrated drive of the system towards a more stable Fe_4N phase. As a consequence of the formation of these structures, nitrogen atoms tend to cluster, reducing their poisoning effect. At the same time, the reduction in the number of catalytic centers is counteracted by an increase in their lifetime. The combined effect is that the barrier for dissociation is not significantly altered at least up to the maximum coverage studied here of 50%.

The Haber-Bosch process is of the greatest economical relevance and arguably one of the major discoveries of the last century [2–4]. Yet in spite of much effort [4–30], its workings are poorly understood. Encouraged by recent progress in *ab initio*-grade simulations [31–39], we have undertaken a long-term project on the Haber-Bosch catalysis. In the first study [1], we simulated the dissociation of N_2 on a clean BCC Fe(111). The (111) surface is indeed the most active one, and the cleavage of the di-nitrogen triple bond has been argued to be its rate-limiting step [4, 5, 7, 27]. In this first investigation, we have discovered a great difference in behavior between low and high temperatures, and have highlighted the dramatic role played by surface dynamics [1, 40, 41]. In particular, already at $T \approx 600$ K, the Fe surface atoms become highly mobile while, at the same time, the long-range order is preserved. This dynamical change has important consequences on the ability of the surface to catalyze the decomposition of the N_2 molecules at *operando* temperatures. In particular, the C_7 centers (Figure 1), that assist the breaking of the N_2 triple bond, acquire a finite lifetime.

Here, we follow Ertl strategy [5] of moving one step at a time towards the full complexity of the Haber-Bosch processes. Thus, leaving the study of the role of H_2 to future investigations, we examine the catalytic properties of the Fe(111) surface after a sizable number of N_2 molecules have been dissociated, and N^* atoms partially cover the surface. At low temperatures, Ertl and collaborators [5] have found that the N^* atoms remain on the surface and order in patterns commensurate with the underlying Fe(111) periodicity. Given that at high temperatures, the surface atoms of the pristine Fe(111) are highly mobile, it is important to ascertain whether this dynamical behavior persists at finite coverage, and

most importantly if and how poisoning is avoided. To this effect, we simulate at room and at the *operando* temperature of 700 K the static, dynamic, and catalytic properties of Fe(111) for N^* coverages of up to 50%. As found in Ref. [1] for the pristine surface, we discover that the catalyst behaves rather differently in these two regimes. At low temperature, poisoning inevitably sets in. In contrast, at the *operando* temperature, poisoning is avoided via a rather intriguing and complex mechanism.

Using the computational workflow developed for the clean surface [1], we construct an *ab initio*-quality machine learning potential optimized to reproduce a wide range of density functional theory (DFT) energy and force calculations [32, 42, 43]. For this procedure to be successful, it is crucial to combine advanced sampling methods [34–37] with active learning procedures to collect all relevant configurations for the entire reaction path under the different conditions studied [1, 44–47]. The synergistic combination of these state-of-the-art methods allows performing large-scale and long-timescale molecular dynamics (MD) simulations of the Fe(111) surface at different N^* atom coverages at room and *operando* temperatures. The procedure used to train and validate the potential is described in detail in the SI Section 1.3, as well as the setup of the simulations [31, 33, 48–56].

Our calculations show that, at finite coverage, the surface loses its long-range order and becomes structurally heterogeneous. New metastable structures appear, which can be described by the formula $Fe_3^*N_i^*$ $i = 1, 4$, where the Fe atoms form an equilateral triangle and sit on top of a vacancy (see Figure 1). This latter positioning is necessary to avoid steric hindrance and is facilitated by the ease with which vacancies can be formed at the *operando* range of temperatures [1]. For the triangular Fe_3^* moiety to be stable, at least one N^* needs to be coordinated to it. The coordinated N^* can sit either at the corner of the Fe_3^* triangle and have five-fold coordination or at its center and have three-fold coordination. The N^* atoms not coordinated to a Fe_3^* moiety are instead four-fold coordinated, and poison the C_7 catalytic centers, see the snapshots in Figure 1. The distribution of the standard and triangular adsorption sites is reported in SI Figure 5. We point out that our potential was able to generalize and predict the existence of these structures. However, given the unexpected nature of these results, we validated them against full-fledged DFT calculations. These confirmed that the presence of a vacancy leads to the formation of the triangular structure Fe_3^* (SI Figure 6), which is stabilized by the presence of adjacent N^* atoms (SI Figure 7).

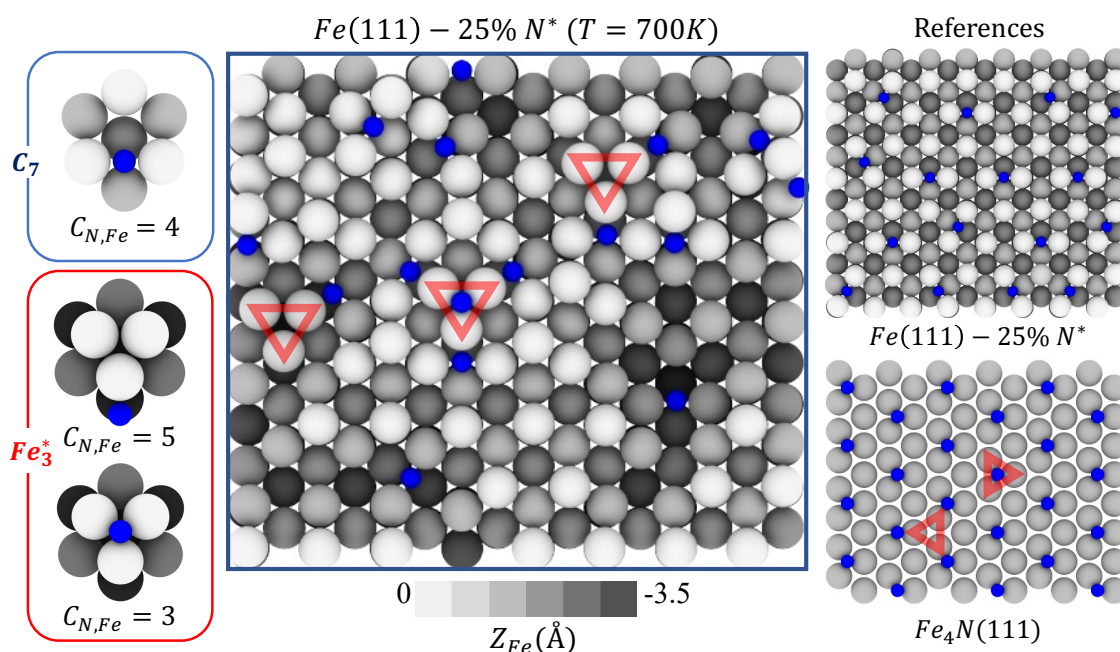


Figure 1: Snapshot of the Fe(111) surface covered with 25% N^* during a molecular dynamics simulation at 700 K (center). The Fe_3^* sites, each surrounded by varying numbers of N^* atoms, are indicated by red triangles. Different coordination environments of N^* are illustrated on the left. In the top right panel, the reference Fe(111) with 25% N^* coverage (initial structure is taken as the one suggested by Bozso et al. [5]) and optimized at 300 K. All N^* occupy four-fold coordinated sites and poison the C_7 sites in this low temperature scenario. Fe atoms are color-coded according to their height along the [111] axis, the N atoms are colored in blue. On the bottom right panel, a picture of the $Fe_4N(111)$ surface is presented and triangles analogous to those observed on the N^* covered BCC Fe(111) surface at 700 K are highlighted.

Furthermore, these triangular motives are characteristic of the $Fe_4N(111)$ surface, which is the nitride phase stable at the *operando* conditions. Thus, the structures observed can be seen as early precursors of an incipient and frustrated transition to the nitride phase. A similar behavior has been experimentally observed during the catalytic decomposition of O_2 on the silver surface [57].

The formation of the $Fe_3^*N_i^*$ complexes induces a clustering of the adsorbate atoms as reflected by the strong short-range correlation between the N^* atoms, see Figure 2 for the 25% coverage and SI Figure 8 for the others. This is evident from the contrast between the distribution of atoms in the standard four-fold coordination and those belonging to the triangular motifs. We also show for comparison the distribution of the N^* distances at room temperature, where atoms remain in their initial ordered structure. In SI Figure 9, we report additional simulation in which the substrate is held at room temperature but the adsorbate atoms are allowed to diffuse by increasing their temperature, obtaining results similar to the four-fold coordinated case. This is a striking evidence of how much the $N^* - N^*$ effective interaction is modulated by the substrate. It also warns against the danger of treating the surface as static, even if the reagents are allowed to move.

The N^* atom clustering around the Fe_3^* triangular motives determines a reduction of the effective N^* surface coverage (see SI Figure 10) in the region free of triangular motives reducing the poisoning effect. This is apparent in SI Figure 11, where the probability of finding an N^* close to a C_7 site is much reduced relative to the 300 K case where N^* atoms are uniformly distributed over the surface.

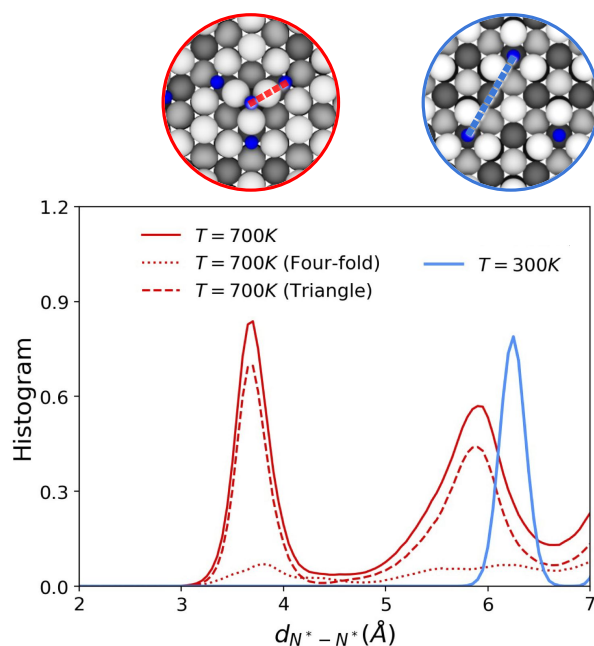


Figure 2: Average distribution of the $N^* - N^*$ distances on the 25% covered Fe(111) surface at 700 K. In the figure are shown the histograms of distances; between all atoms (solid red line), between all pairs of atoms in which at least one is coordinated to a Fe_3^* triangle (dashed line), and between uncoordinated atoms ($C_{N,Fe} = 4$) using dotted line. We also contrast the $N^* - N^*$ histogram at 700 K (solid red line) with the corresponding histogram at 300 K (solid blue line). Above the picture, we report two snapshots highlighting the distances that contribute to the dominant peaks at low and high temperatures.

Having briefly described the structural changes induced by N^* , we focus on the dynamical properties of the surface. The atoms involved in the $Fe_3^*N_i^*$ motifs have a slower dynamics compared to the other atoms. As a result, the average iron diffusion decreases with coverage while remaining sizable (SI Figure 12); this allows surface dynamics to affect the system behavior also at finite coverage. As the concentration of N^* increases, the density of the Fe_3^* triangles increases while that of the C_7 -like environments (henceforth denoted as χ_7) decreases, as can be seen in Figure 3 (top panel). Both surface features have a finite lifetime, as reported in Figure 3 (bottom panel). The lifetime distributions are non-Gaussian, with long tails towards long lifetimes. It is important for the system catalytic activity that the average lifetime of the χ_7 catalytic environments increases as a function of coverage.

We then studied how this complex dynamics affects the ability of the N^* -covered surface to adsorb and dissociate an incoming N_2 molecule. In Ref. [1], we found that two collective variables could well describe the behavior of

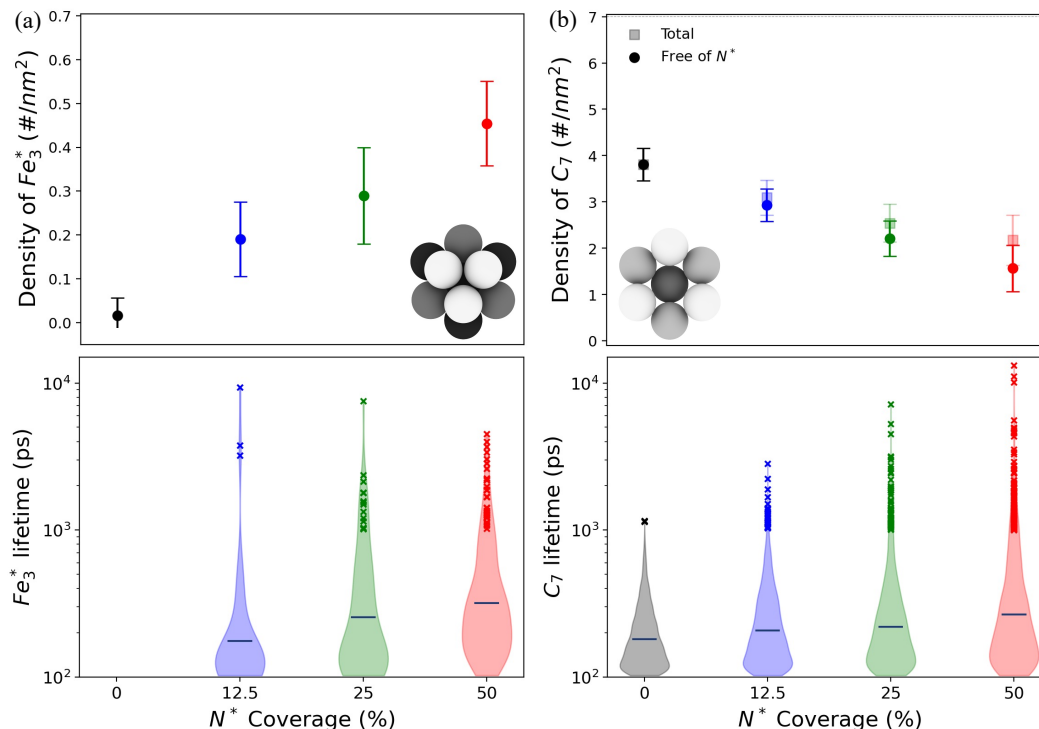


Figure 3: Surface density and violin plot of lifetime distribution for a) Fe_3^* and b) C_7 sites. These are calculated using the Environment Similarity [58] as described in the SI Section 1.5.1. For the surface density of C_7 , faded squares indicate the overall density of C_7 , while solid circles denote the density of C_7 sites unaffected by N^* poisoning. In the lifetime distribution plots, only Fe_3^* and C_7 sites with lifetimes of at least 100 ps are considered. Sites with lifetimes surpassing 1 ns are indicated by x markers.

this process; the N_2 bonding length d and the charge transferred from the metallic surface to the nitrogen molecule q [59–64]. Changes in q are a rather reliable indicator of the underlying chemical process and allow classifying the absorption states without having to specify explicitly the N_2 's geometrical arrangement. The q values were computed by training a graph neural network on the data collected in Ref. [1] supplemented by the new ones obtained here for the covered surface, see SI Section 1.6. It is remarkable that the very same variables can be used profitably also in the more complex situation described here, as can be seen in Figure 4, where we compare the free energy $F(d, q)$ at 300 K and 700 K for a coverage of 25% N^* . See also SI Section 2.2.1 for the free energies at the other coverages and SI Section 2.2.2 for an analysis of the available reaction pathways. At $T = 300$ K, one can recognize the classical adsorption sites of the low-temperature studies of nitrogen chemisorption on iron [4, 7, 25]. As the charge transfer increases, the adsorption sites go from a vertical γ/δ to a horizontal α , and to the precursor horizontal α' state in which the molecule sits in the second layer just above the C_7 iron atoms. At $T = 700$ K, the overall qualitative behavior is similar with the notable exception of the instability of the α' state due to the surface dynamics, already noted in Ref. [1] for the clean surface.

A more quantitative and punctual comparison between the systems at different temperatures and coverages can be made via the minimum free energy paths on the space (d, q) which are very little dependent on the system studied (see SI Section 2.2). In this representation, the difference in behavior between the low and the high-temperature behavior is striking. In the $T = 300$ K case, where the atom mobility is close to zero and the surface structure is ordered, the free energy barrier between the α state and dissociation increases with coverage reflecting the poisoning effect of the N^* atoms, in agreement with Ertl experiments [5]. In striking contrast, at $T = 700$ K, the free energy barrier hardly changes, at least within the range of concentrations studied here, see Figure 4. Two main physical effects conspire to yield this result: the surface atoms mobility, which is reduced but not quenched by the N^* and the looming transition to a nitride phase. The former pushes the lifetime of the C_7 sites to higher values while the latter leads to the formation of $Fe_3^*N_i^*$ complexes and to a clustering of N^* atoms reducing the number of poisoning nitrogen, see Figure 3. This compensates the decrease in available χ_7 environments, leading only to very small changes in the free energy barrier.

In conclusion, our simulations show that the overall catalytic activity of the Fe(111) surface is due not only to the existence of catalytic sites, but also to the properties of the surface as a whole, its dynamics and its fluctuations. The closeness to a phase transition toward the nitride phase helps inducing the kind of heterogeneous static and dynamical behavior observed here and sustaining the fluctuations needed for the catalytic process to be stabilized. A beneficial effect on the catalyst resistance to poisoning comes from a combination of surface dynamics and chemical processes-induced changes. Similar observations of the dramatic effects of surface dynamics and reaction-induced changes can be found in the literature, with notable examples being the activation of the copper surface by carbon monoxide [65] and the destabilization of lithium imide surfaces under ammonia decomposition [47]. Our study demonstrates that a static description of one such catalyst is inadequate as suggested some time ago by Spencer [40], when he argued that for an industrial catalyst to be as stable as it is, a steady state dynamical process needs to be set up. He did indicate two possible ways in which this can happen, either the surface atoms become mobile or the reaction itself changes dynamically the surface. One can recognize that in this process the two scenarios combine in one. Finally, we note that the picture depicted here could be experimentally checked with modern *operando* surface spectroscopy techniques and these experiments could also be used for studying the nucleation of the nitride phase [65, 66].

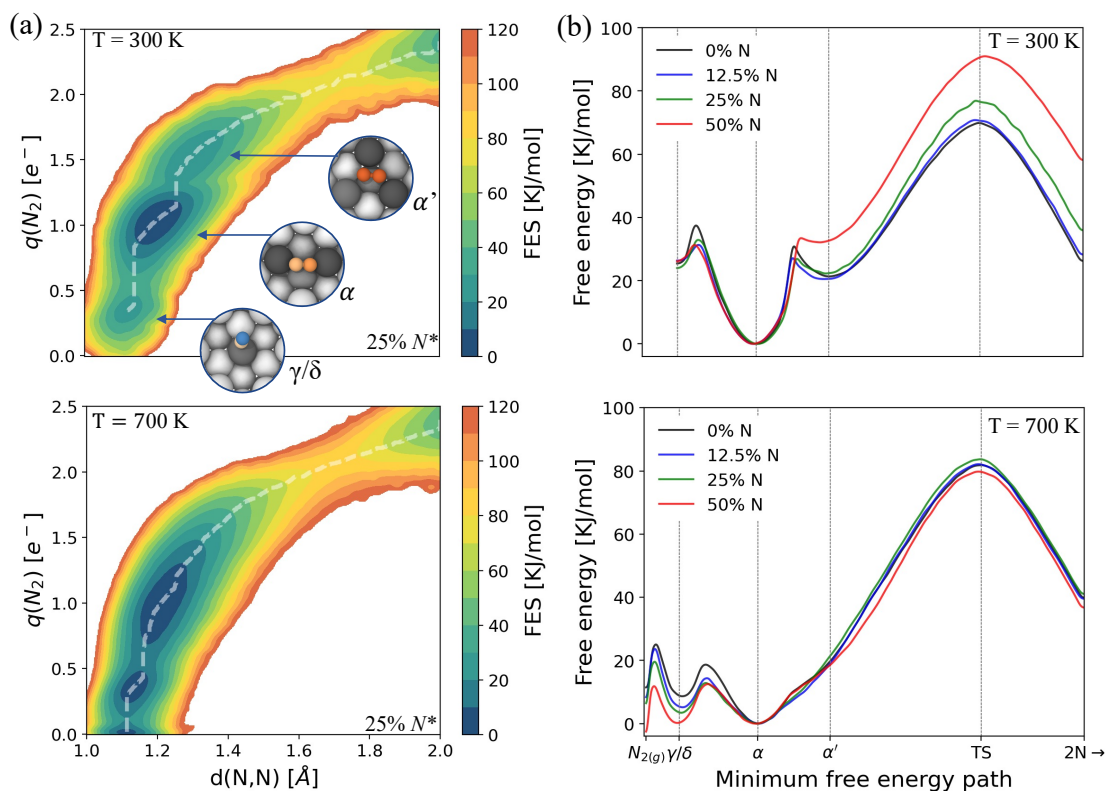


Figure 4: (a) The free energy, $F(d, q)$ is plotted as a function of N-N distance and the nitrogen charge $q(N_2)$ (defined as the sum of the partial charges of N atoms) at 300 K and 700 K for a surface covered with 25% N^* . Results for the other concentrations are reported in SI Figures 12-13. The local minima on the plots correspond to metastable states, and the white dashed lines indicate the minimum free energy pathway (s_m) in this plane. The snapshots of various adsorption sites (γ/δ , α , and α') are shown in the top panel of (a). (b) The minimum free energy profile ($F(s_m)$) computed along the s_m in $d - q$ space for the Fe(111) surface at 300 K and 700 K. In plotting the $T = 700$ K, we have not considered those transitions that take place on the Fe_3^* triangles whose energy barrier is much higher (120 kJ/mol) than the one associated with the C_7 sites. See SI Figure 17 for the free energy profiles computed using all pathways. The reference is set to 0 for the lowest energy state (α). Note that, for 10 bar N_2 partial pressure, we do not find $N_2(g)$ to be a metastable state at 300 K.

Acknowledgements We are thankful to Pierdomenico Biasi, Rene Eckert, Cristina Pizzolitto, Daniela Polino, Stephan Reitmeier, Beatriz Roldán Cuenya, Umberto Raucci, and Robert Schögl for insightful discussions. In particular, M.P. is indebted to Robert Schögl for generously sharing his understanding of catalysis. Calculations were performed on

the Cineca Marconi100 cluster under project id IsB26 and on the IIT cluster Franklin. We acknowledge the CINECA award under the ISCRA initiative and the help of the Franklin Support Team at the Italian Institute of Technology.

References

- [1] L. Bonati et al. “The role of dynamics in heterogeneous catalysis: surface diffusivity and N_2 decomposition on Fe(111)”. In: (2023).
- [2] F. Haber. “The synthesis of ammonia from its elements”. In: *Nobel Lecture 2* (1920).
- [3] J. W. Erisman, M. A. Sutton, J. Galloway, Z. Klimont, and W. Winiwarter. “How a century of ammonia synthesis changed the world”. In: *Nature geoscience* 1.10 (2008), pp. 636–639.
- [4] G. A. Somorjai and N. Materer. “Surface structures in ammonia synthesis”. In: *Topics in Catalysis* 1.3-4 (1994), pp. 215–231.
- [5] F. Bozso, G. Ertl, M. Grunze, and M. Weiss. “Interaction of nitrogen with iron surfaces: I. Fe (100) and Fe (111)”. In: *Journal of Catalysis* 49.1 (1977), pp. 18–41.
- [6] D. Strongin. “The importance of C7 sites and surface roughness in the ammonia synthesis reaction over iron”. In: (1986).
- [7] J. J. Mortensen et al. “Nitrogen adsorption on Fe (111),(100), and (110) surfaces”. In: *Surface science* 422.1-3 (1999), pp. 8–16.
- [8] A. Logadottir and J. K. Nørskov. “The effect of strain for N_2 dissociation on Fe surfaces”. In: *Surface science* 489.1-3 (2001), pp. 135–143.
- [9] R. Egeberg et al. “ N_2 dissociation on Fe (1 1 0) and Fe/Ru (0 0 0 1): what is the role of steps?” In: *Surface science* 491.1-2 (2001), pp. 183–194.
- [10] I. Goikoetxea, M. Alducin, R. D. Muiño, and J. Juaristi. “Dissociative and non-dissociative adsorption dynamics of N_2 on Fe (110)”. In: *Physical Chemistry Chemical Physics* 14.20 (2012), pp. 7471–7480.
- [11] S. C. Yeo, S. S. Han, and H. M. Lee. “Adsorption, dissociation, penetration, and diffusion of N_2 on and in bcc Fe: first-principles calculations”. In: *Physical Chemistry Chemical Physics* 15.14 (2013), pp. 5186–5192.
- [12] A. J. Medford et al. “Assessing the reliability of calculated catalytic ammonia synthesis rates”. In: *Science* 345.6193 (2014), pp. 197–200.
- [13] I. Goikoetxea, J. Juaristi, R. D. Muiño, and M. Alducin. “Surface Strain Improves Molecular Adsorption but Hampers Dissociation for N_2 on the Fe/W (110) Surface”. In: *Physical Review Letters* 113.6 (2014), p. 066103.
- [14] L. Xu, D. Kirvassilis, Y. Bai, and M. Mavrikakis. “Atomic and molecular adsorption on Fe (110)”. In: *Surface Science* 667 (2018), pp. 54–65.
- [15] B.-Y. Zhang, H.-Y. Su, J.-X. Liu, and W.-X. Li. “Interplay Between Site Activity and Density of BCC Iron for Ammonia Synthesis Based on First-Principles Theory”. In: *ChemCatChem* 11.7 (2019), pp. 1928–1934.
- [16] G. Ertl, S. Lee, and M. Weiss. “Adsorption of nitrogen on potassium promoted Fe (111) and (100) surfaces”. In: *Surface Science* 114.2-3 (1982), pp. 527–545.
- [17] J.-L. Shi, S.-Q. Xiang, W. Zhang, and L.-B. Zhao. “A thermodynamic and kinetic study of the catalytic performance of Fe, Mo, Rh and Ru for the electrochemical nitrogen reduction reaction”. In: *Physical Chemistry Chemical Physics* 22.44 (2020), pp. 25973–25981.
- [18] D. Liu, W. Zhao, and Q. Yuan. “Breaking the Linear Relation in the Dissociation of Nitrogen on Iron Surfaces”. In: *ChemPhysChem* 23.17 (2022), e202200147.
- [19] M. Muhler, F. Rosowski, and G. Ertl. “The dissociative adsorption of N_2 on a multiply promoted iron catalyst used for ammonia synthesis: a temperature-programmed desorption study”. In: *Catalysis letters* 24 (1994), pp. 317–331.
- [20] P. Stoltze and J. Nørskov. “The surface science based ammonia kinetics revisited”. In: *Topics in Catalysis* 1 (1994), pp. 253–263.
- [21] R. Schlögl, R. Schoonmaker, M. Muhler, and G. Ertl. “Bridging the “material gap” between single crystal studies and real catalysis”. In: *Catalysis letters* 1 (1988), pp. 237–241.
- [22] J. Scholten, P. Zwietering, J. Konvalinka, and J. De Boer. “Chemisorption of nitrogen on iron catalysts in connection with ammonia synthesis. Part 1.—The kinetics of the adsorption and desorption of nitrogen”. In: *Transactions of the Faraday Society* 55 (1959), pp. 2166–2179.
- [23] J. Scholten and P. Zwietering. “Kinetics of the chemisorption of nitrogen on ammonia—synthesis catalysts”. In: *Transactions of the Faraday Society* 53 (1957), pp. 1363–1370.
- [24] P. Zwietering and J. Roukens. “The kinetics of the chemisorption of nitrogen on iron catalysts”. In: *Transactions of the Faraday Society* 50 (1954), pp. 178–187.
- [25] G. Ertl, S. Lee, and M. Weiss. “Kinetics of nitrogen adsorption on Fe (111)”. In: *Surface Science* 114.2-3 (1982), pp. 515–526.
- [26] I. Alstrup, I. Chorkendorff, and S. Ullmann. “The interaction of nitrogen with the (111) surface of iron at low and at elevated pressures”. In: *Journal of Catalysis* 168.2 (1997), pp. 217–234.
- [27] N. Spencer, R. Schoonmaker, and G. Somorjai. “Iron single crystals as ammonia synthesis catalysts: effect of surface structure on catalyst activity”. In: *Journal of Catalysis* 74.1 (1982), pp. 129–135.
- [28] M. Weiss, G. Ertl, and F. Nitschke. “Adsorption and decomposition of ammonia on Fe (110)”. In: *Applications of Surface Science* 2.4 (1979), pp. 614–635.

- [29] G. Ertl. “Primary steps in catalytic synthesis of ammonia”. In: *Journal of Vacuum Science & Technology A: Vacuum, Surfaces, and Films* 1.2 (1983), pp. 1247–1253.
- [30] M.-C. Tsai, U. Ship, I. Bassignana, J. Küppers, and G. Ertl. “A vibrational spectroscopy study on the interaction of N₂ with clean and K-promoted Fe (111) surfaces: π -bonded dinitrogen as precursor for dissociation”. In: *Surface science* 155.2-3 (1985), pp. 387–399.
- [31] P. Giannozzi et al. “QUANTUM ESPRESSO: a modular and open-source software project for quantum simulations of materials”. In: *Journal of physics: Condensed matter* 21.39 (2009), p. 395502.
- [32] J. Behler and M. Parrinello. “Generalized neural-network representation of high-dimensional potential-energy surfaces”. In: *Physical review letters* 98.14 (2007), p. 146401.
- [33] H. Wang, L. Zhang, J. Han, and E. Weinan. “DeePMD-kit: A deep learning package for many-body potential energy representation and molecular dynamics”. In: *Computer Physics Communications* 228 (2018), pp. 178–184.
- [34] O. Valsson, P. Tiwary, and M. Parrinello. “Enhancing important fluctuations: Rare events and metadynamics from a conceptual viewpoint”. In: *Annual review of physical chemistry* 67 (2016), pp. 159–184.
- [35] A. Laio and M. Parrinello. “Escaping free-energy minima”. In: *Proceedings of the national academy of sciences* 99.20 (2002), pp. 12562–12566.
- [36] A. Barducci, G. Bussi, and M. Parrinello. “Well-tempered metadynamics: a smoothly converging and tunable free-energy method”. In: *Physical review letters* 100.2 (2008), p. 020603.
- [37] M. Invernizzi and M. Parrinello. “Rethinking metadynamics: From bias potentials to probability distributions”. In: *The journal of physical chemistry letters* 11.7 (2020), pp. 2731–2736.
- [38] L. Grajciar et al. “Towards operando computational modeling in heterogeneous catalysis”. In: *Chemical Society Reviews* 47.22 (2018), pp. 8307–8348.
- [39] G. Piccini et al. “Ab initio molecular dynamics with enhanced sampling in heterogeneous catalysis”. In: *Catalysis Science & Technology* 12.1 (2022), pp. 12–37.
- [40] M. Spencer. “Stable and metastable metal surfaces in heterogeneous catalysis”. In: *Nature* 323.6090 (1986), pp. 685–687.
- [41] R. Schlögl. “Heterogeneous catalysis”. In: *Angewandte Chemie International Edition* 54.11 (2015), pp. 3465–3520.
- [42] O. T. Unke et al. “Machine Learning Force Fields”. In: *Chemical Reviews* 121.16 (2021), pp. 10142–10186.
- [43] L. Zhang, J. Han, H. Wang, R. Car, and E. Weinan. “Deep potential molecular dynamics: a scalable model with the accuracy of quantum mechanics”. In: *Physical review letters* 120.14 (2018), p. 143001.
- [44] L. Bonati and M. Parrinello. “Silicon liquid structure and crystal nucleation from ab initio deep metadynamics”. In: *Physical review letters* 121.26 (2018), p. 265701.
- [45] H. Niu, L. Bonati, P. M. Piaggi, and M. Parrinello. “Ab initio phase diagram and nucleation of gallium”. In: *Nature communications* 11.1 (2020), p. 2654.
- [46] M. Yang, L. Bonati, D. Polino, and M. Parrinello. “Using metadynamics to build neural network potentials for reactive events: the case of urea decomposition in water”. In: *Catalysis Today* 387 (2022), pp. 143–149.
- [47] M. Yang, U. Raucci, and M. Parrinello. “Reactant-induced dynamics of lithium imide surfaces during the ammonia decomposition process”. In: *Nature Catalysis* (2023), pp. 1–8.
- [48] G. Bussi, D. Donadio, and M. Parrinello. “Canonical sampling through velocity rescaling”. In: *The Journal of chemical physics* 126.1 (2007), p. 014101.
- [49] P. Giannozzi et al. “Advanced capabilities for materials modelling with Quantum ESPRESSO”. In: *Journal of physics: Condensed matter* 29.46 (2017), p. 465901.
- [50] P. Giannozzi et al. “Quantum ESPRESSO toward the exascale”. In: *The Journal of chemical physics* 152.15 (2020), p. 154105.
- [51] J. P. Perdew, K. Burke, and M. Ernzerhof. “Generalized gradient approximation made simple”. In: *Physical review letters* 77.18 (1996), p. 3865.
- [52] A. M. Rappe, K. M. Rabe, E. Kaxiras, and J. Joannopoulos. “Optimized pseudopotentials”. In: *Physical Review B* 41.2 (1990), p. 1227.
- [53] N. Marzari, D. Vanderbilt, A. De Vita, and M. Payne. “Thermal contraction and disordering of the Al (110) surface”. In: *Physical review letters* 82.16 (1999), p. 3296.
- [54] H. J. Monkhorst and J. D. Pack. “Special points for Brillouin-zone integrations”. In: *Physical review B* 13.12 (1976), p. 5188.
- [55] S. Plimpton. “Fast parallel algorithms for short-range molecular dynamics”. In: *Journal of computational physics* 117.1 (1995), pp. 1–19.
- [56] G. A. Tribello, M. Bonomi, D. Branduardi, C. Camilloni, and G. Bussi. “PLUMED 2: New feathers for an old bird”. In: *Computer physics communications* 185.2 (2014), pp. 604–613.
- [57] B. Andryushechkin, V. Shevlyuga, T. Pavlova, G. Zhidomirov, and K. Eltsov. “Adsorption of O₂ on Ag (111): evidence of local oxide formation”. In: *Physical Review Letters* 117.5 (2016), p. 056101.
- [58] P. M. Piaggi and M. Parrinello. “Calculation of phase diagrams in the multithermal-multibaric ensemble”. In: *The Journal of chemical physics* 150.24 (2019).
- [59] R. F. Bader. “Atoms in molecules”. In: *Accounts of Chemical Research* 18.1 (1985), pp. 9–15.
- [60] G. Henkelman, A. Arnaldsson, and H. Jónsson. “A fast and robust algorithm for Bader decomposition of charge density”. In: *Computational Materials Science* 36.3 (2006), pp. 354–360.

- [61] K. T. Schütt, H. E. Sauceda, P.-J. Kindermans, A. Tkatchenko, and K.-R. Müller. “SchNet—a deep learning architecture for molecules and materials”. In: *The Journal of Chemical Physics* 148.24 (2018), p. 241722.
- [62] K. Schütt et al. “SchNetPack: A deep learning toolbox for atomistic systems”. In: *Journal of chemical theory and computation* 15.1 (2018), pp. 448–455.
- [63] D. P. Kingma and J. Ba. “Adam: A method for stochastic optimization”. In: *arXiv preprint arXiv:1412.6980* (2014).
- [64] I. Marcos-Alcalde, J. Setoain, J. I. Mendieta-Moreno, J. Mendieta, and P. Gomez-Puertas. “MEPSA: minimum energy pathway analysis for energy landscapes”. In: *Bioinformatics* 31.23 (2015), pp. 3853–3855.
- [65] B. Eren et al. “Activation of Cu (111) surface by decomposition into nanoclusters driven by CO adsorption”. In: *Science* 351.6272 (2016), pp. 475–478.
- [66] M. Salmeron and R. Schlögl. “Ambient pressure photoelectron spectroscopy: A new tool for surface science and nanotechnology”. In: *Surface Science Reports* 63.4 (2008), pp. 169–199.